



# Systematic $H_\infty$ weighting function selection and its application to the real-time control of a vertical take-off aircraft

Jiankun Hu<sup>a,\*</sup>, Christian Bohn<sup>b</sup>, H.R. Wu<sup>c</sup>

<sup>a</sup>Department of Computer Systems Engineering, RMIT University, Melbourne 3000, Australia

<sup>b</sup>Control Engineering Laboratory, Department of Electrical Engineering and Information Technology, Ruhr-University Bochum, D 44780 Bochum, Germany

<sup>c</sup>School of Computer Science & Software Engineering, Monash University, Australia

Received 21 July 1998; accepted 10 August 1999

## Abstract

In this paper, the selection of  $H_\infty$  weighting functions for general practical applications is investigated. It is shown that an  $H_\infty$  weighting function for a single-input–single-output (SISO) plant can be obtained by considering a series of connections of elementary low-order plants. For a constrained control effort, an explicit weighting function expression is derived for the first time. A novel method for the selection of weighting functions in  $H_\infty$  mixed sensitivity design is proposed to control the percentage overshoot directly. An example illustrating how the transient response of a standard  $H_\infty$  design is improved by using the proposed weighting functions is provided. Finally, real-time experimental results are presented for the roll-angle control of a laboratory-scale physical model of a vertical take-off aircraft. © 2000 Elsevier Science Ltd. All rights reserved.

**Keywords:**  $H_\infty$  control; Weighting functions; Real-time control; Aircraft control

## 1. Introduction

In practical applications of  $H_\infty$ -optimal control, one of the major difficulties is how to select suitable weighting functions that incorporate both stability and performance requirements. The results of the design will depend strongly on these weighting functions, no matter what kind of algorithm is used to compute the controller. Some interesting results on this topic are found in the literature (Postlethwaite, O'Young, Gu & Hope, 1987; Postlethwaite, Tsai & Gu, 1990; Garg & Ouzts, 1991; Garg, 1993; Kiffmeier & Unbehauen, 1993; Kiffmeier, 1994; Yang, Ju & Liu, 1994a; Yang, Tsai & Lee, 1994b; Knepova, Kiffmeier & Unbehauen, 1995; Hu, Unbehauen & Bohn, 1996; Hu, Bohn & Wu, 1999; to name just a few). Unfortunately, no explicit formula to choose weighting functions is proposed, except in the works of Garg (1993), Hu et al. (1996, 1999). Instead, weighting functions are usually determined experimentally to meet performance specifications (see, for example, Yang et al., 1994a, b; Knepova et al., 1995). However, for a practical

design problem the choice is not trivial, which hinders the great potential of the  $H_\infty$  control approach in real-life applications. Therefore, the best way would be to provide a basic form for the weighting functions that reflect basic system specifications, and, more importantly, that gives designers a simple way to do trade-offs. In light of this, the work in this paper does not intend to provide a universal formula for all cases, nor does it provide a simple trial and error method. Instead, it provides explicit formulae for typical plants that more complicated cases have roots in. They may serve as a good starting point even in a very sophisticated  $H_\infty$  design task. The work presented here is an extension of the work in Hu et al. (1996, 1999).

The problem of the high order of the resulting controller is alleviated by a balanced realization model reduction technique (Moore, 1981). Other interesting topics, such as systematic  $H_\infty$  weighting function selection for unmodeled dynamics, disturbances, and advanced model reduction techniques for high-order  $H_\infty$  controllers, are not addressed in this paper. Conventional methods are simply adopted whenever these issues are encountered. For a more in-depth discussion of these issues, interested readers may refer to the listed references (Garg & Ouzts, 1990; Garg, 1993).

\* Corresponding author. Tel.: +61-3-992-55316; fax +61-3-992-55340.

E-mail address: jiankun.hu@rmit.edu.au (J. Hu)

The remainder of this paper is organized as follows. In Section 2, uncertainty weights for typical low-order plants are derived. Then it is shown that an explicit formula can be directly obtained for a general *SISO* plant that consists of these elementary low-order plants. In Section 3, an explicit weighting function expression is derived to take into account actuator position and rate constraints, assuming that the delay term is approximated by a first-order Pade expansion. Then, a basic form is suggested for the weighting function. Using this approach, the system steady-state performance and bandwidth can be adjusted independently, which is superior to the popular approach of “Constrained  $H_\infty$  Control Design” (CHCD) (Postlethwaite et al., 1987, 1990). Furthermore, a novel procedure is proposed to modify the weighting function in order to control the percentage overshoot directly. In Section 4, the method presented here is elaborated upon by a roll-angle control design of a laboratory scale vertical take-off aircraft (with nonlinear characteristics neglected). A comparison is made by using the standard  $H_\infty$  design method and the method proposed in this paper. The results of a real-time control experiment with a controller obtained by the proposed method is also presented. Section 5 is devoted to the conclusion.

**2. Weighting functions for parametric uncertainties**

From an engineering point of view, it is extremely difficult to give an explicit and versatile formula or to set direct rules on how to choose  $H_\infty$  weighting functions, due to the enormous variety of different practical problems. However, many complex systems can often be considered as a combination of equivalent and typical low-order plants. Providing some definite rules for some of these plants will certainly be of great interest to control engineers. The plants that will be discussed in this section are a first-order lag ( $PT_1$ ), a first-order plus dead time process ( $PT_{1t}$ ), a second-order system with real poles and dead time ( $PT_{2t}$ ), and second-order oscillatory system ( $PT_{2s}$ ). The extension to general *SISO* plants is also discussed.

*2.1. Preliminaries*

To begin with, consider a standard mixed sensitivity *S/R/T* design (Postlethwaite et al., 1987) shown in Fig. 1.  $W_e(s)$ ,  $W_u(s)$ , and  $W_y(s)$  are weighting functions for the sensitivity matrix function  $S(s)$ , the control signal sensitivity matrix function  $R(s)$ , and the complementary sensitivity matrix  $T(s)$ , respectively, where  $S = (1 + GC)^{-1}$ ,  $R = CS$ ,  $T = GC(1 + GC)^{-1}$  and  $S + T = 1$ .  $G$  is the plant, and  $C$  is the controller. The mixed sensitivity

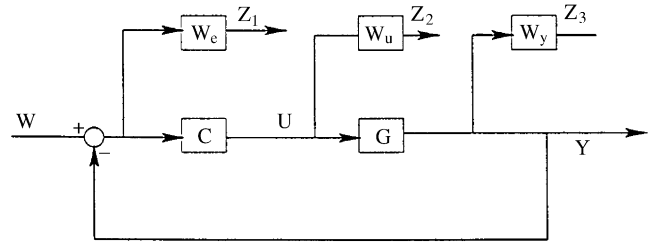


Fig. 1. Mixed sensitivity *S/R/T* design.

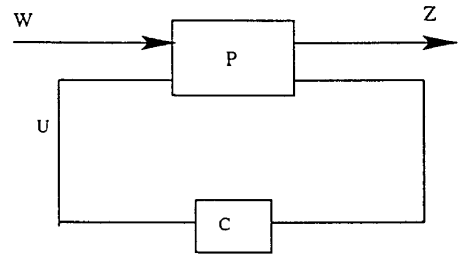


Fig. 2. General  $H_\infty$  control problem.

*S/R/T* design is formulated as

$$\|F(P, C)\|_\infty = \left\| \begin{bmatrix} W_s S \\ W_u R \\ W_y T \end{bmatrix} \right\|_\infty < 1, \tag{1}$$

where  $P$ ,  $C$  are depicted in a general  $H_\infty$  control problem shown in Fig. 2, and  $P$  represents the generalized plant (Doyle, Glover, Khargonekar & Francis, 1990)

$$P(s) = \begin{bmatrix} P_{11} & P_{12} \\ P_{21} & P_{22} \end{bmatrix} = \begin{bmatrix} C_1 \\ C_2 \end{bmatrix} (sI - A)^{-1} [B_1 B_2] + \begin{bmatrix} D_{11} & D_{12} \\ D_{21} & D_{22} \end{bmatrix}. \tag{2}$$

*2.2.  $H_\infty$  weighting function selection*

Throughout this paper, the “DGKF” (Doyle et al., 1990) algorithm is used to compute  $H_\infty$ -optimal controllers. Typical plants  $PT_1$ ,  $PT_{1t}$ ,  $PT_{2t}$ , and  $PT_{2s}$  are investigated first. For simple typical *SISO* plants  $PT_1$ ,  $PT_{1t}$ , and  $PT_{2t}$  with parametric uncertainties, it is not difficult to verify that the weighting functions given in Table 1 can cover the uncertainty.

Now, consider a more complex  $PT_{2s}$  plant given by

$$G(s) = \frac{K\omega_n^2}{\omega_n^2 + 2d\omega_n s + s^2}, \tag{3}$$

where  $K$  is the steady-state gain,  $d$  is the damping factor, and  $\omega_n$  is the natural frequency. The following

Table 1  
Weighting functions for elementary plants with parametric uncertainties

Plant ( $PT_1$ )	$G(s) = \frac{K}{Ts + 1}$	Uncertainty	$K_0 - \Delta K_0 \leq K \leq K_0 + \Delta K_0$ $T_0 - \Delta T_0 \leq T \leq T_0 + \Delta T_0$
Weigh. Fun.	$W_y(s) = \frac{(\Delta K_0 T_0 + K_0 \Delta T_0)s + \Delta K_0}{K_0[(T_0 - \Delta T_0)s + 1]}$		
Plant ( $PT_{1\tau}$ )	$G(s) = \frac{Ke^{-\tau s}}{Ts + 1}$	Uncertainty	$K_0 - \Delta K_0 \leq K \leq K_0 + \Delta K_0$ $\tau_0 - \Delta \tau_0 \leq \tau \leq \tau_0 + \Delta \tau_0$ $T_0 - \Delta T_0 \leq T \leq T_0 + \Delta T_0$
Weigh. Fun.	$W_y(s) = \frac{\Delta K_0 + [K_0(\tau_0 + \Delta T_0) + \Delta K_0(T_0 + 0.5\Delta \tau_0)]s - (2K_0 T_0 + \Delta K_0 T_0 + K_0 \Delta T_0) \frac{\Delta \tau_0}{2} s^2}{K_0[(T_0 - \Delta T_0)s + 1]}$		
Plant ( $PT_{2\tau}$ )	$G(s) = \frac{Ke^{-\tau s}}{(T_1 s + 1)(T_2 s + 1)}$	Uncertainty	$K_0 - \Delta K_0 \leq K \leq K_0 + \Delta K_0$ $T_{10} - \Delta T_{10} \leq T_1 \leq T_{10} + \Delta T_{10}$ $T_{20} - \Delta T_{20} \leq T_2 \leq T_{20} + \Delta T_{20}$ $\tau_0 - \Delta \tau_0 \leq \tau \leq \tau_0 + \Delta \tau_0$
Weigh. fun.	$W_y(s) = \frac{\Delta K_0 + a_1 s + a_2 s^2 + a_3 s^3}{b(s)}$  $a_1 = \Delta K_0(T_{10} + T_{20}) + \frac{\Delta \tau_0}{2}(K_{\max} + K_0) + K_0(\Delta T_{10} + \Delta T_{20})$ $a_2 = -\Delta K_0 T_{10} T_{20} - K_0 \Delta T_{10} T_{20} - K_0 T_{10} \Delta T_{20} - K_0 \Delta T_{10} \Delta T_{20}$ $- [K_{\max}(T_{10} + T_{20}) + K_0(T_{1\max} + T_{2\max})] \frac{\Delta \tau_0}{2}$ $a_3 = -\frac{\Delta \tau_0}{2}(K_{\max} T_{10} T_{20} + K_0 T_{1\max} T_{2\max})$ $b(s) = K_0[(T_{10} - \Delta T_{10})s + 1][(T_{20} - \Delta T_{20})s + 1].$		

uncertainties are assumed

$$K_0 - \Delta K_0 \leq K \leq K_0 + \Delta K_0,$$

$$d_0 - \Delta d_0 \leq d \leq d_0 + \Delta d_0,$$

$$\omega_{n0} - \Delta \omega_{n0} \leq \omega_n \leq \omega_{n0} + \Delta \omega_n. \tag{4}$$

The multiplicative error becomes

$$\frac{G - G_0}{G_0} = \frac{\Delta K + 2(Kd_0/\omega_{n0} - K_0 d/\omega_n)s + (K/\omega_{n0}^2 - K_0/\omega_n^2)s^2}{K_0(1 + 2(d/\omega_n)s + (1/\omega_n^2)s^2)}. \tag{5}$$

The general shape of the amplitude  $|(G - G_0)/G_0|$  of (5) for varying values of all three parameters  $K$ ,  $\omega_n$ , and  $d$  is shown in Fig. 3 by the dotted curve.

To construct an uncertainty weighting function, the starting point would be an upper bound in the frequency region up to the first peak. One simple way is to find an approximate peak. A weighting function that acts as such an upper bound for this peak is found by substituting the lowest natural frequency, the smallest damping into the denominator of (5) and using the upper bound of the

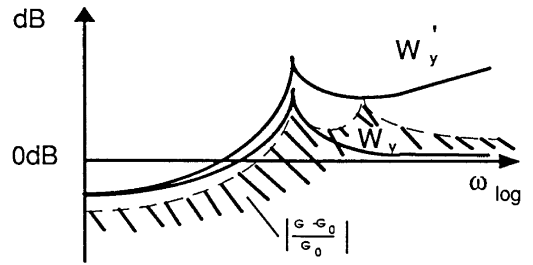


Fig. 3. Uncertainty region and upper bound.

numerator of (5), which leads to

$$W_y(s) = \frac{\Delta K_0 + p_1 s + p_2 s^2}{K_0(1 + 2[(d_0 - \Delta d_0)/(\omega_{n0} - \Delta \omega_{n0})]s + [1/(\omega_{n0} - \Delta \omega_{n0})^2]s^2)},$$

$$p_1 = \frac{2[\Delta K_0 \omega_{n0} d_0 + K_0 \Delta \omega_{n0} d_0 + \Delta K_0 \Delta \omega_{n0} d_0 + K_0 \omega_{n0} \Delta d_0]}{\omega_{n0}(\omega_{n0} - \Delta \omega_{n0})},$$

$$p_2 = \frac{K_0 - \Delta K_0}{\omega_{n0}^2} - \frac{K_0}{\omega_{n0} - \Delta \omega_{n0}}. \tag{6}$$

To modify the uncertainty weighting function  $W_y$  so that it will cover the whole frequency, two extra zeros are added. Hence, it results in the new uncertainty weighting function

$$W'_y(s) = W_y(s)(Ts + 1)^2. \tag{7}$$

The two additional zeros are chosen so that the modified weighting function becomes almost exactly the upper bound, and thus includes the peak of the maximum uncertainty at the highest frequency. Here, this highest peak can be obtained approximately by substituting the highest natural frequency  $\omega_{nmax}$ , the smallest damping  $d_{min}$ , and the maximum gain  $K_{max}$  into (6) and by finding the frequency at which the resulting transfer function attains this peak. As a result, (6) becomes

$$\frac{\Delta K_0 + 2(K_{max} d_0/\omega_{n0} - K_0 d_{min}/\omega_{nmax})s + (K_{max}/\omega_{n0}^2 - K_0/\omega_{nmax}^2)s^2}{K_0(1 + 2(d_{min}/\omega_{nmax})s + (1/\omega_{nmax}^2)s^2)} = \frac{\alpha_0 + \alpha_1 s + \alpha_2 s^2}{\beta_1 + \beta_2 s + \beta_3 s^2} = E'(s), \tag{8}$$

and for  $s = j\omega$

$$|E'(j\omega)|^2 = \frac{\alpha_1^2 \omega^2 + (\alpha_0 - \alpha_2 \omega^2)^2}{\beta_1^2 \omega^2 + (\beta_0 - \beta_2 \omega^2)^2}. \tag{9}$$

To find the peak point, let  $x = \omega^2$  and set

$$f(x) = \frac{\alpha_1^2 x + (\alpha_0 - \alpha_2 x)^2}{\beta_1^2 x + (\beta_0 - \beta_2 x)^2}, \tag{10}$$

$$\frac{df}{dx} = 0 \Leftrightarrow Ax^2 + Bx + C = 0, \tag{11}$$

where

$$A = (\beta_1 \alpha_2)^2 - \beta_2^2 (\alpha_1^2 - 2\alpha_0 \alpha_2) - 2\beta_0 \beta_2 \alpha_2^2,$$

$$B = 2(\beta_0 \alpha_2)^2 - 2(\beta_2 \alpha_0)^2,$$

$$C = \beta_0^2 (\alpha_1^2 - 2\alpha_0 \alpha_2) + 2\alpha_0^2 \beta_2 \beta_0 - (\alpha_0 \beta_1)^2.$$

Therefore, the maximal peak frequency is given by

$$\omega_{pr} = \sqrt{\frac{-B + \sqrt{B^2 - 4AC}}{2A}}. \tag{12}$$

To satisfy  $|W'_y(j\omega_{pr})| = |E'(j\omega_{pr})|$ ,  $T$  is obtained as

$$T = \frac{1}{\omega_{pr}} \sqrt{\frac{|E'(j\omega_{pr})|}{|W_y(j\omega_{pr})|} - 1}. \tag{13}$$

Many simulation examples demonstrate that the uncertainty weighting covers the uncertainty region as shown in Fig. 3.

*Extension to a general SISO plant:* Obviously, a general SISO plant can always be obtained by a product of the following elementary units (D'Azzo & Houpis, 1995):

- (i)  $K$ ,
- (ii)  $e^{-ts}$ ,
- (iii)  $1/(Ts + 1)$ ,

- (iv)  $Ts + 1$ ,
- (v)  $\omega_n^2/(\omega_n^2 + 2d\omega_n s + s^2)$ ,
- (vi)  $(s^2 + 2d\omega_n s + \omega_n^2)/\omega_n^2$ ,
- (vii)  $1/s$ ,
- (viii)  $s$ .

Items (i)–(iii) can be replaced by one  $PT_{1r}$  unit. The uncertainty weighting functions for these elementary units are either given in the previous sections or can be obtained by a minor modification of the given results. Assume that a general SISO plant with parameter uncertainties is expressed by

$$G(s) = \frac{K(T_1 s + 1)e^{-\tau s} \omega_n^2 \dots}{s^m (T_2 s + 1)(s^2 + 2d\omega_n s + \omega_n^2) \dots}, \tag{14}$$

or more generally

$$G(s) = \frac{1}{s^m} \prod_{i=1}^n g_i(s), \tag{15}$$

where  $g_i(s)$  is one of the above-defined elementary units. Let

$$G(s) = G_0(s)(1 + W_y \Delta) \|\Delta\|_\infty \leq 1, \tag{16}$$

$$g_i(s) = g_{i0}(1 + W_{yi} \Delta_i) \|\Delta_i\|_\infty \leq 1, \tag{17}$$

as shown in Fig. 4.

The general plant with parameter uncertainty can be expressed as (15).

This yields

$$\begin{aligned} G_0(s)(1 + W_y \Delta) &= \frac{1}{s^m} \prod_{i=1}^n g_{i0}(1 + W_{yi} \Delta_i) \\ &= \frac{1}{s^m} \left( \prod_{i=1}^n g_{i0} \right) (1 + W_{y1} \Delta_1 + W_{y2} \Delta_2 \\ &\quad + W_{y1} W_{y2} \Delta_1 \Delta_2 + \dots). \end{aligned} \tag{18}$$

Since

$$\Delta \Leftrightarrow \Delta_1 \Leftrightarrow \Delta_2 \Leftrightarrow \dots \Leftrightarrow \Delta_n \Leftrightarrow \Delta_1 \Delta_2 \Leftrightarrow \dots, \tag{20}$$

from (19), it holds that

$$G_0(s) = \frac{1}{s^m} \prod_{i=1}^n g_{i0}. \tag{21}$$

Then the weighting function is obtained as

$$W_y(s) = \prod_{i=1}^n (1 + W_{yi}(s)). \tag{22}$$

**Remark 1.** Many high-order systems are physically composed of these elementary components. No extra effort is needed for decomposition in these cases. When an intact physical component does not belong to any one of these elementary components, it can be decomposed into an individual elementary unit. Such decomposition resembles mode separation. Each mode normally corresponds to a type of physical phenomenon. There are many

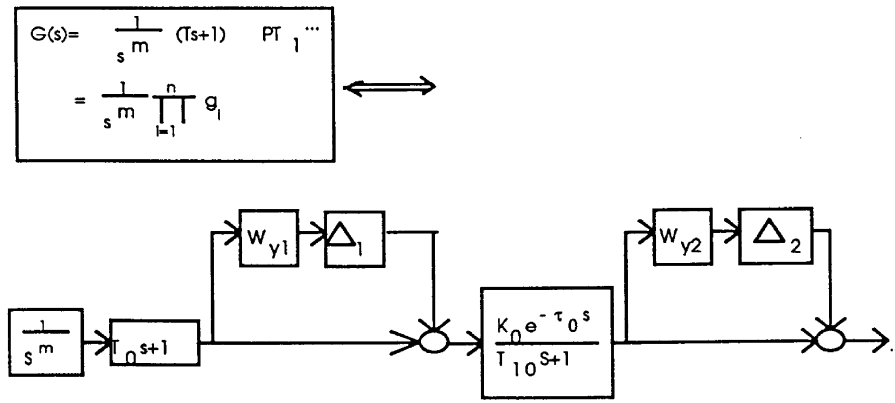


Fig. 4. Decomposition of a general SISO plant.

high-order systems that fit this structure nicely. Here are a few practical examples: a typical fifth-order tape-drive system; a fourth-order system for the lateral and longitudinal control of a Boeing 747 (Franklin, Powell & Naeni, 1994); a fourth-order system for the position control of a space-vehicle camera (D’Azzo & Houpis, 1995). In fact, the Bode plot method uses the same decomposition technique for the identification and control of high-order systems (D’Azzo & Houpis, 1995). One advantage of this decomposition technique in constructing the weighting function is that physical phenomena can be reflected at mode-level.

**Remark 2.** It is very difficult to provide an explicit weighting function for a high-order system with parametric uncertainties. In the scheme proposed here, as indicated by (22), an explicit weighting function is derived by simple multiplication and addition once a decomposition is carried out as indicated in Remark 1.

**3. A new approach to  $H_\infty$  weighting function selection**

In engineering applications, the percentage steady-state error  $e_\infty$  is commonly used to represent the steady-state performance requirements. The important transient performance requirements include the rise time, the overshoot, and the settling time. The goal, therefore, is to select appropriate and versatile weighting functions to portray these requirements.

*3.1. Performance weighting function selection*

For a plant without an integrator, the following form for  $W_e(s)$  is suggested

$$W_e(s) = \lambda \frac{s + \rho_1^\mu}{s + \tau_1}, \quad \mu \in \{0, 1\}. \tag{23}$$

When the parameter  $\mu$  is set to 1, the formula  $1/\lambda = 1/W_e(\infty)$  represents the amplification factor of a disturbance at high frequencies, that is, the disturbance rejection ability of the system at high frequencies.  $e_\infty = 1/W_e(0) = \tau_1/\lambda\rho_1$  is the steady-state error (if zero steady-state error is required,  $\tau_1$  must be chosen as zero). Parameter  $\mu$  will be set to zero when a high-frequency disturbance is not considered. Obviously, with the increase of  $\rho_1$ ,  $e_\infty$  will decrease. For transient behavior, no general formulae that express the dependence between the overshoot/rise time and the frequency response are available. All that is known is that the response time is roughly inversely proportional to the bandwidth, and the overshoot depends on the peak magnitude and the roll-off rate of the frequency response.

Let  $\omega_e$  be the crossover frequency of  $W_s(s)$  and  $\omega_b$  the bandwidth, then

$$\omega_e \approx \omega_b \sqrt{\frac{2(\lambda\rho_1)^2 - \tau_1^2}{1 - 2\lambda^2}}, \quad \lambda < \frac{1}{\sqrt{2}}. \tag{24}$$

In practice, one can increase  $\rho_1$  to get the widest possible bandwidth. When the plant has a  $\phi$ -multiple integrator, (23) should be altered. From (1),  $\|W_e S\|_\infty = \|W_e(I + GK)^{-1}\|_\infty < 1$ , then in (23),  $\tau_1$  should be 0,  $W_e(s)$  should have at least a  $\phi$ -multiple pole at the origin, otherwise the sensitivity  $S(s)$  at low frequencies cannot be shaped. If  $W_e(s)$  has a  $\gamma$ -multiple pole at the origin, then the resulting  $H_\infty$  controller would possess a  $(\gamma - \phi)$ -multiple integrator. The attention of the reader is now drawn to the following point. For simplicity, consider the following weighting function:

$$W_e(s) = \lambda \frac{s + \rho_1}{s}. \tag{25}$$

In this case, the difference between the method proposed and the aforementioned CHCD is portrayed in Figs. 5 and 6. The widely used CHCD is shown in Fig. 5. During the design phase, the parameter  $\rho_1$  is kept fixed, and the parameter  $\lambda$  is increased as much as possible. This would

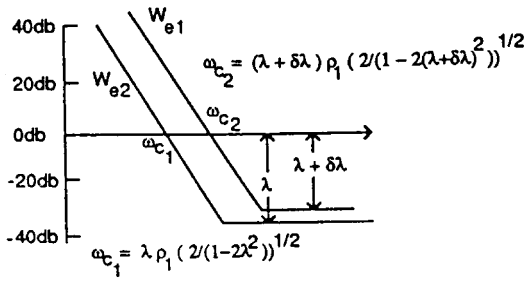


Fig. 5. CHCD tuning:  $\lambda$  is increased while  $\rho_1$  is fixed ( $\tau_1 = 0$ ).

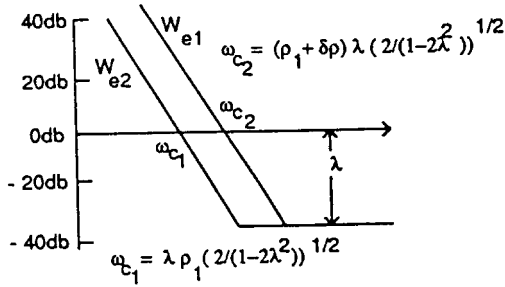


Fig. 6. Proposed method:  $\rho_1$  is increased while  $\lambda$  is fixed at each stage ( $\tau_1 = 0$ ).

simultaneously force the system bandwidth and the disturbance attenuation ability of the system at high frequencies to increase in an unknown and interrelated way, rendering contradictory results, i.e., there would be an improvement of one criterion at the expense of the deterioration of another one. In Fig. 6, the adjustment of system bandwidth and disturbance attenuation at high frequencies are separate. It is all-too-natural for control engineers to make bandwidth as wide as possible, observing, of course, other physical constraints and the stability requirements imposed by the uncertainty weighting function. Designers could make easy trade-offs with this method.

### 3.2. Selection of the controlled signal weighting function $W_u(s)$

Practically, an actuator always has position and rate limit constraints. Hence, it is important to use a suitable weighting function to represent these constraints. This problem has already been addressed by several authors (Postlethwaite et al., 1987, 1990; Garg & Ouzts, 1991; Garg, 1993; Kiffmeier & Unbehauen, 1993; Kiffmeier, 1994; Yang et al., 1994a, b; Kneppova et al., 1995; Hu et al., 1996, 1999, to name just a few), but no direct result or explicit formula has been given except in the works of Garg (1993), Hu et al. (1996, 1999). Garg (1993) has modified the cost function of the conventional mixed sensitivity design by augmenting the normal control sensitivity function  $R(s)$  with an additional control signal rate function. In this paper, a simple, definite weighting

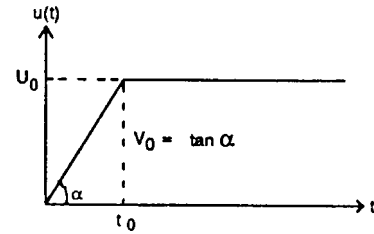


Fig. 7. Characteristic response of the actuator signal  $u(t)$  due to a step input of magnitude  $m$ .

function is proposed to incorporate both position and rate limits without changing the cost function of the conventional mixed sensitivity design. It is assumed that the delay can be approximated by a first-order expansion. Suppose that the maximal position of an actuator is  $U_0$  and its rate limit is  $V_0$ . Assume that these constraints should be met when the system is subject to a step input of magnitude  $m$ . Then, one can choose a special  $u(t)$ , a limit response to a step input of magnitude  $m$ , to cover all possible control signals as illustrated in Fig. 7.

From Fig. 7, it follows that

$$u(t) = \begin{cases} V_0 t, & 0 \leq t \leq t_0, \\ U_0, & t_0 \leq t \leq \infty. \end{cases} \quad (26)$$

Then, the Laplace-transformation of  $u(t)$  is given by

$$U(s) = \int_0^\infty u(t)e^{-st} dt = \frac{V_0}{s^2} - \frac{V_0}{s^2} e^{-t_0 s}, \quad t_0 = \frac{U_0}{V_0}. \quad (27)$$

Using the first-order Pade approximation

$$e^{-st_0} \approx \left(1 - \frac{st_0}{2}\right) / \left(1 + \frac{st_0}{2}\right) \quad (28)$$

yields

$$U(s) = \frac{U_0}{s} \left(1 + \frac{U_0}{2V_0}s\right)^{-1}. \quad (29)$$

It is obvious that

$$\begin{aligned} \frac{1}{s} mR(s) &= \frac{U_0}{s(1 + (U_0/2V_0)s)} \rightarrow R(s) \\ &= \frac{U_0/m}{1 + (U_0/2V_0)s}. \end{aligned} \quad (30)$$

Therefore, referring to (1), the control signal weighting function could be chosen as

$$W_u(s) = \frac{m}{U_0} \left(1 + \frac{U_0}{2V_0}s\right). \quad (31)$$

When only a maximal bound, i.e.,  $|u(t)| \leq U_0$ , is required,  $V_0$  should be set to  $\infty$ , which gives

$$W_u(s) = \frac{m}{U_0}. \quad (32)$$

This process possesses a physical interpretation that is clearly shown in Fig. 7. Since a step input is the most commonly used signal, the weighting function expressed by (31) is very useful. For other types of input signals, they can be viewed as filtered outputs of a step input. Obviously, the transfer function of this filter can be obtained as  $s\mathcal{L}\{Input\}$ , where  $\mathcal{L}\{\cdot\}$  is a Laplace-transformation.

The authors are aware that from a mathematical point of view (31) might not hold for all cases. This is because from  $|X_1(j\omega)| \geq |X_2(j\omega)|$  one cannot generally infer that  $x_1(t) \geq x_2(t)$ . Instead, one would have to check the positive definiteness of  $X_1(j\omega) - X_2(j\omega)$  to guarantee  $x_1(t) - x_2(t) \geq 0$  (Solodownikov, 1971). Nevertheless, the approach under discussion should still be used since (31) should hold for many practical problems. This is because the control signal weighting function is required to describe two factors, namely the maximum position bound  $U_0$  and the maximum speed  $V_0$ . The simple form of (31) could meet these requirements in most cases. For the maximal bound requirement  $U_0$ , this is obvious. It is known that the response time (rise, or settling time) is inversely proportional to the bandwidth (or the cross-over frequency) of the transfer function. From Fig. 7, the response has the shortest response time, i.e., (31) has possibly the highest cross-over frequency or corner frequency. This means that all control signal responses with a maximal speed less than  $V_0$  and/or response time less than that of Fig. 7 are mostly covered by (31). On the other hand, simulations are always an integral part of any control system's design, and for the cases in which this procedure might fail, (31) might still serve as a good starting point for the selection of a weighting function.

### 3.3. Direct control of percentage overshoot

Although the steady-state performance can be easily translated into the plot of  $G_w(j\omega)$ , this does not hold for the transient-response performance specifications. For a simple second-order system

$$G_w(s) = \frac{\omega_0^2}{s^2 + 2d\omega_0 s + \omega_0^2}, \tag{33}$$

the relationship between the percentage overshoot of the step response and the peak magnitude of the frequency response is given by

$$e_{\max} = \exp\left(-|G_w|_{\max} \pi \left(1 - \sqrt{1 - \frac{1}{|G_w|_{\max}^2}}\right)\right), \tag{34}$$

which can easily be verified to be a monotonously increasing function. When the peak magnitude  $|G_w|_{\max}$  of the frequency response decreases, the damping ratio  $d$  will increase, causing the overshoot  $e_{\max}$  to decrease. From (33), the minimum value of the peak magnitude  $|G_w|_{\max}$  of the frequency is equal to 1, so the minimum

percentage value of overshoot  $e_{\max}$  can be as small as 4.3% by pressing down the peak magnitude  $|G_w|_{\max}$  of the frequency response. The transient response of a complex system can often be considered the result of an equivalent second-order system, and this approximate solution is especially sufficient for determining the peak overshoot (D'Azzo & Houpis, 1995). On this basis, (34) holds approximately for a general system with a dominating pair of poles.

To obtain good performance, high open-loop gain at low frequency is needed. Note that the complementary sensitivity function

$$T(s) = \frac{G(s)K(s)}{1 + G(s)K(s)} \tag{35}$$

is nearly equal to 1 at very low frequencies, i.e.,  $T(j0) = 1$  when integral action is used. Referring to (35), with the replacement of the closed-loop transfer function  $G_w(s)$  by  $T(s)$ , and given the allowable maximum step response overshoot  $e_{\max}$ , if one makes the inequality

$$|T(j\omega)|_{\max} \leq \frac{\pi^2 + \ln(e_{\max}^2)}{2\pi \ln(1/e_{\max})} \tag{36}$$

hold, then, an overshoot smaller than (or close to)  $e_{\max}$  is guaranteed. This is possible because  $|T(j\omega)|_{\max}$  always appears below the crossover frequency  $\omega_y$ . Below this region, the uncertainty weight  $W_y(s)$  is relatively small, and  $|T(j\omega)|$  is close to 1. This means that the uncertainty weight  $W_y(s)$  has little, or even no influence on the complementary sensitivity  $T(s)$  in this region. In most practical cases,  $W_y(s)$  is used to represent the unmodeled dynamics uncertainty, which is usually large at high frequencies. And at low frequencies, uncertainty could be made small. Therefore, one has the potential to change the ‘‘uncertainty weight’’  $W_y(s)$  within this frequency region, while keeping the resulting mixed-sensitivity design close to the original one. The procedures of controlling the closed-loop system overshoot are summarized as follows.

*Transient performance control procedure (TPCP):* (1) Select the weighting functions  $W_e(s)$ ,  $W_u(s)$ , and  $W_y(s)$ ,

(2) Given the overshoot  $e_{\max}$ , calculate the maximum allowable complementary sensitivity  $|T(j\omega)|_{\max}$  using (36), then change the weighting function  $W_y(s)$  to  $W'_y(s)$  so that

$$1 \geq \min_{\omega \in \Theta} |W'_y(j\omega)| \geq \frac{1}{|T(j\omega)|_{\max}}, \tag{37}$$

where  $\Theta$  is the frequency region below  $\omega_e$  in which  $|T(j\omega)|_{\max}$  may occur and  $W'_y(s)$  is made close to  $W_y(s)$  over the crossover frequency  $\omega_y$  of  $W_y(s)$ ,

(3) Increase the parameter  $\rho_1$  (or parameter  $\lambda$  when  $\mu$  equals zero) in  $W_e(s)$  as much as possible using available  $H_\infty$  software, i.e., increase the bandwidth  $\omega_b$  as much as possible to get the fastest response.

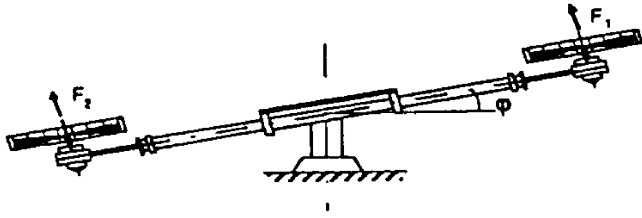


Fig. 8. Schematic diagram of the pilot plant.

**4. Roll-angle control of a laboratory scale vertical take-off aircraft**

*4.1. Description of the plant*

The positioning of a heavy beam by means of two propellers, as shown in Fig. 8, is a non-trivial example for testing control strategies. The controlled variable is the angle  $\phi$  formed with the horizontal line. The input variable of the controlled system, which is also the manipulating signal, is the command voltage  $u$  for the power amplifiers of the DC-motors driving the propellers. In a linearized description, the dynamic behavior between the input voltage of the amplifier and the speed  $n$  of the propeller attached to the shaft of the motor, can be described by a first-order lag, representing the dynamic behavior of an independently excited DC-motor. Neglecting friction, integration of the angular acceleration of the beam  $\ddot{\phi}$  aroused by moment  $M$  yields the angular velocity, and further integration generates the angle  $\phi$ . The non-linear characteristics between the motor speed  $n$  and the generated moment  $M$  are introduced by the propeller mechanism. Neglecting the non-linearity in Fig. 9, the system can be described by

$$G(s) = \frac{b}{s^2(s + \alpha)}, \tag{38}$$

where  $b = K_A K_\phi K_M / (J T_M)$  and  $\alpha = 1/T_M$ .

*4.2.  $H_\infty$  controller design*

For the selected nominal plant,  $\alpha = 3.02, b = -6.84$ , the uncertainty weighting function  $W_y(s)$  could be chosen as

$$W_y(s) = 0.46(0.965s + 1) \tag{39}$$

by experiment (Kiffmeier, 1994). The plant has a double integrator and hence is not stable. As discussed in the previous section, the performance weighting function

$$W_e(s) = \frac{\lambda}{s^2} \tag{40}$$

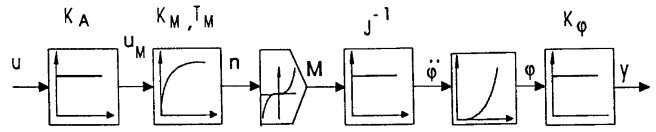


Fig. 9. Input-output block diagram of the plant.

is selected. Here, a scaling factor of 0.6 which acts on the sensitivity function  $S(s)$  is absorbed by the parameter  $\lambda$ . For the mixed  $S/R/T$  design, as stated in step 3 of the described algorithm in Section 3, the performance weighting function is simply kept unchanged as expressed by (40). This sensitivity weighting function violates the condition of observability and detectability due to the double pure integrator if the “DGKF” algorithm is used. This difficulty can be overcome by replacing  $s$  in the integrator by  $(s + \epsilon)$ , where  $\epsilon$  is a small positive number. This modification has little influence on the actual design because it keeps sensitivity weighting at low frequencies sufficiently large, which is the goal of using a pure integrator.

Now, the normalized control-signal magnitude constraint  $|u(t)| \leq 0.5$  is assumed for a square wave input with a normalized amplitude of  $\pm 0.3$ , and an overshoot of less than 6.5% is required. From (31),  $W_u(s) = 0.6/0.5$  is simply chosen.

*4.2.1. Standard  $H_\infty$  design method*

For standard  $H_\infty$  design, the uncertainty weighting function  $W_y(s)$  does not go through the modification step outlined in procedure TPCP. The controller is obtained as a fifth-order transfer function

$$K(s) = \frac{569.84s^4 + 1880.84s^3 + 482.98s^2 + 9.659 \times 10^{-3}s + 4.829 \times 10^{-8}}{s^5 + 688.79s^4 + 3413.26s^3 + 5340.29s^2 + 10.67s + 5.33 \times 10^{-3}} \tag{41}$$

The singular value plot of the cost function is shown in Fig. 10.

The all-pass characteristics at low frequency that decreases at high frequency indicates a typically successful  $H_\infty$  design in the sense that a sub-optimal  $H_\infty$  controller is obtained for the given weighting functions (Postlethwaite et al., 1987, 1990). The corresponding complementary sensitivity and the inverse of the uncertainty weighting function are shown in Fig. 11. It is clear that the complementary sensitivity  $T$  has a bad shape indicating a large overshoot. Output and control-signal time responses to the square-wave input specified are shown in Figs. 12 and 13. A bad transient performance with more than 30% overshoot is obtained.

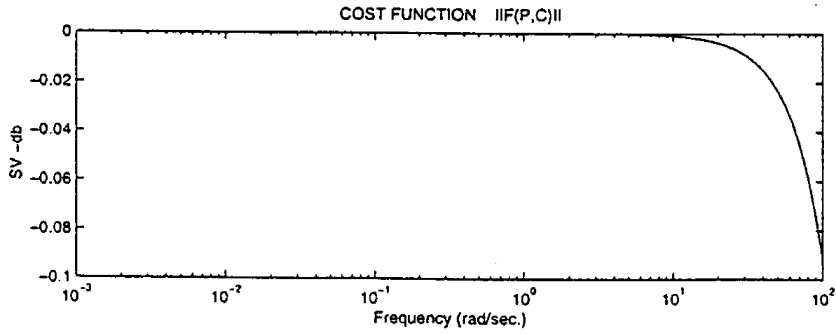


Fig. 10. Singular-value plot of the weighted mixed sensitivity using the standard  $H_\infty$  design.

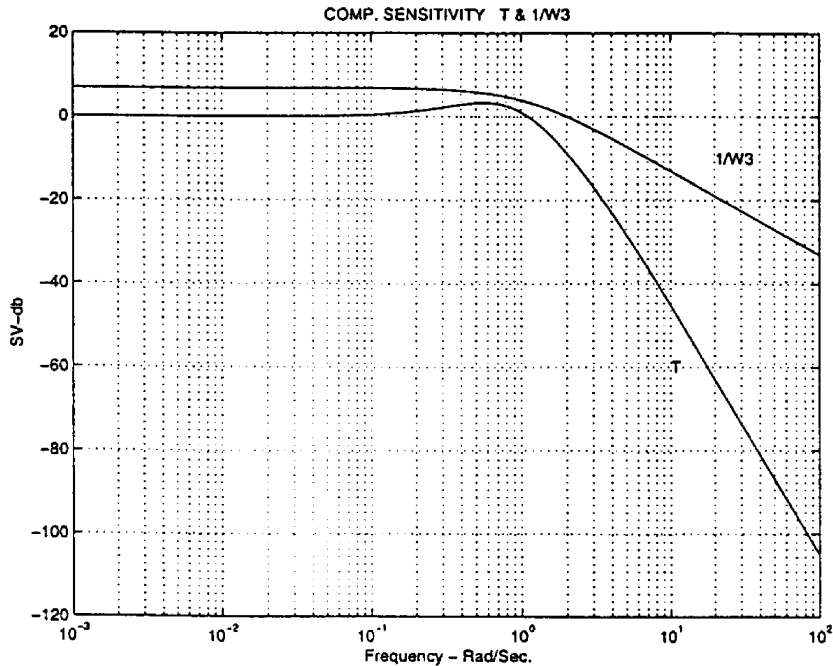


Fig. 11. Singular-value plots of the complementary sensitivity and the inverse of the uncertainty weighting function using the standard  $H_\infty$  design.

4.2.2. Proposed  $H_\infty$  design

Referring to (37), for the control of the overshoot,  $W_y(s)$  is changed to

$$W'_y(s) = \frac{31.82s^4 + 107.76s^3 + 48.13s^2 + 0.123s + 7.9 \times 10^{-5}}{106.45s^3 + 67.39s^2 + 14.22s + 1} \quad (42)$$

From Fig. 14, it holds that  $|W'_y(j\omega)| \leq 1.0097$  within the frequency range  $\omega \in [0.0109, \infty]$ . When the peak of the complementary sensitivity  $T(s)$  appears in this region, an overshoot of less than 6.5% will be guaranteed. To satisfy the constant rank condition on the  $j\omega$ -axis (Doyle et al., 1990), two extra zeros that lie far beyond the system bandwidth are added to give  $W'_y(s) = W'_y(0.001s + 1)^2$ .

Using the “Hinf” toolbox of *Matlab*,  $\lambda$  is increased to get as wide as possible a bandwidth. It should be pointed

out that the “DGKF” algorithm can often raise various numerical problems, especially in solving Riccati equations. Generally, this phenomena becomes extremely serious when the solution approaches optimality. In this example, the numerical problem arises mainly because of the double integrator used. Numerical analysis shows that the matrix  $A$  of the general plant  $[A \ B_1 \ B_2 \ C_1 \ C_2 \ D_{11} \ D_{12} \ D_{21} \ D_{22}]$  has a high condition number,  $cond(A) = 1.84 \times 10^{19}$ . As a remedy, a scaling technique is introduced,

$$A' = diag^{-1}(\Gamma) \times A \times diag(\Gamma), \quad B'_i = diag^{-1}(\Gamma)B_i \quad (43)$$

$$C'_i = C_i \cdot diag(\Gamma), \quad i = 1, 2 \quad (44)$$

where  $\Gamma$  is a scaling vector.  $\Gamma$  should be selected so that all the elements in the new matrix  $A'$  are as close as possible. Or, one can use the uniformly distributed

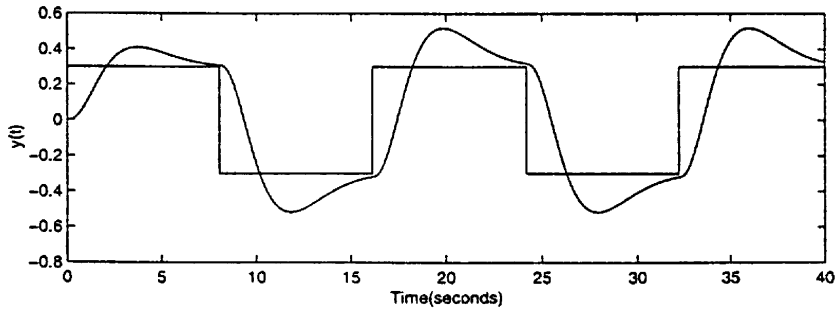


Fig. 12. Output response tracking a square wave of magnitude  $\pm 0.3$  using the standard  $H_\infty$  design.

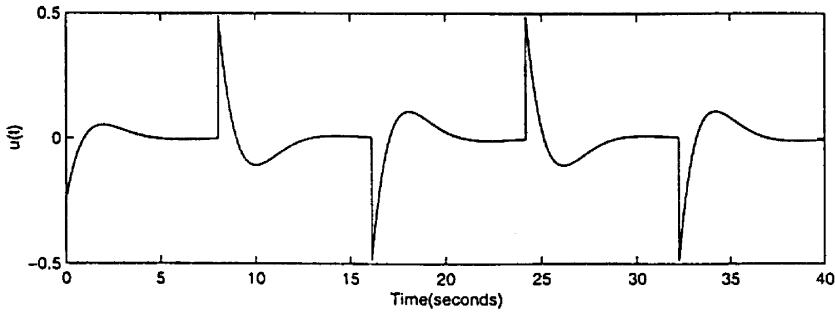


Fig. 13. Control signal response using the standard  $H_\infty$  design.

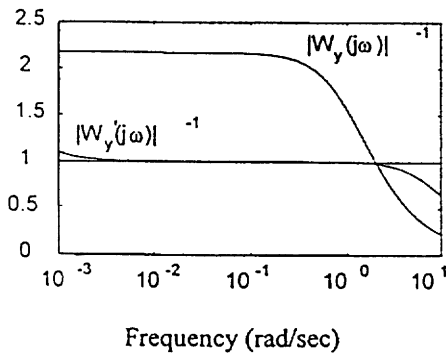


Fig. 14. Changed uncertainty weighting.

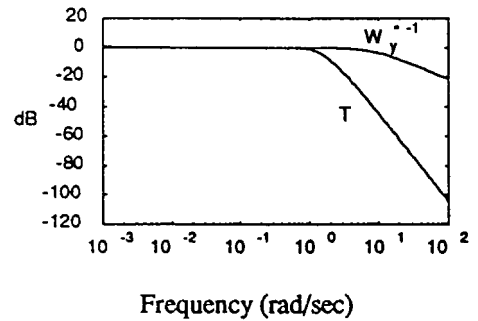


Fig. 15. Singular-value plots of  $T$  and  $W_y'(s)^{-1}$  using the proposed method.

random number generator function *rand* in *MATLAB* to generate a smaller condition number matrix  $A'$ . Here, the latter method is used, and the condition number  $cond(A')$  is decreased to  $10^{16}$ . With the largest parameter,  $\lambda = 9.873e - 4$ , a seventh-order sub-optimal  $H_\infty$  controller is obtained. After model reduction using a balanced realization technique (Moore, 1981), a third-order  $H_\infty$  controller with the transfer function

$$K(s) = -\frac{0.83s^3 + 2.52s^2 + 2.45 \times 10^{-2}s + 8.75 \times 10^{-6}}{s^3 + 4.92s^2 + 7.52s + 0.023} \quad (45)$$

is obtained.

From Figs. 15 and 16, the peak magnitude 1.0087 of  $T(j\omega)$  appears at 0.094 (rad/s), which is within the frequency range  $[0.0109, \infty]$ . By using (36), the percentage overshoot should be smaller than 6.4%. Figs. 17 and 18 show simulation results without a disturbance. The percentage overshoot  $e_{max}$  is 5.76%, which is smaller than and close to the assigned value of 6.4%, and the maximal amplitude of the control signal is 0.484 which is smaller than and close to the bound value of 0.5. All these results verify the effectiveness of the proposed approach. Figs. 19(a)–(d) show the responses of the output and control signal under an additional output step disturbance of amplitude 0.24 with different initial acting times. A good disturbance rejection property is demonstrated. The transient performance of a standard  $H_\infty$  design has

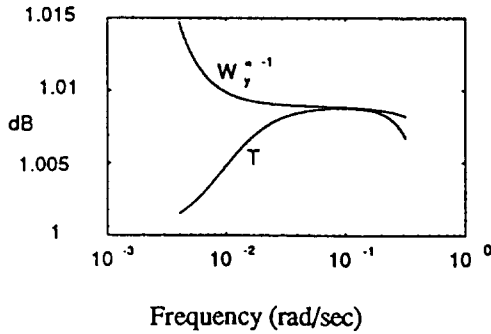


Fig. 16. Magnitude plots of  $T$  and  $W_y(s)^{-1}$  using the proposed method.

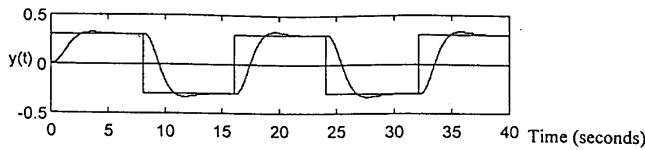


Fig. 17. Output response tracking a square wave of magnitude  $\pm 0.3$  by the proposed method.

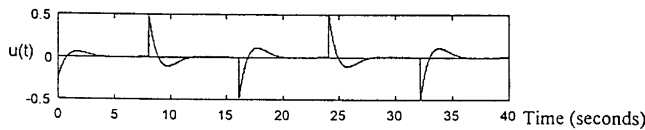


Fig. 18. Control signal response by the proposed method.

been significantly improved by the method proposed in the paper.

#### 4.2.3. Real-time experiment

In addition to the simulation result shown above, a real-time experiment was also conducted for the proposed method on the device at the Control Laboratory of Ruhr University. The hardware host is an IBM PC. A 16 bit A/D, D/A converter board was used. The real-time software “CADACS” (Schmid & Jamshidi, 1996) has been used. This real-time PC-version toolbox was written using Turbo Pascal 4.0 and contains, besides the real-time routines, five program examples, including all libraries in source format. The user writes his own real-time task using either Borland C or Pascal language. For the choice of sampling rate, the sampling period is less than or equal to  $\frac{1}{20}$  of the system bandwidth. The system bandwidth was less than 1 (rad/s), hence, a sampling rate of 0.01 (s) and a zero-order hold were chosen. Two machine attached knobs that tuned the rotation of each propeller separately were used to set the operating point. The experimental results are shown in Figs. 20(a) and (b). In Fig. 20(a), the overshoot is about 8%, the rise time is about 2.2 s, and the settling time is about 5 s. In

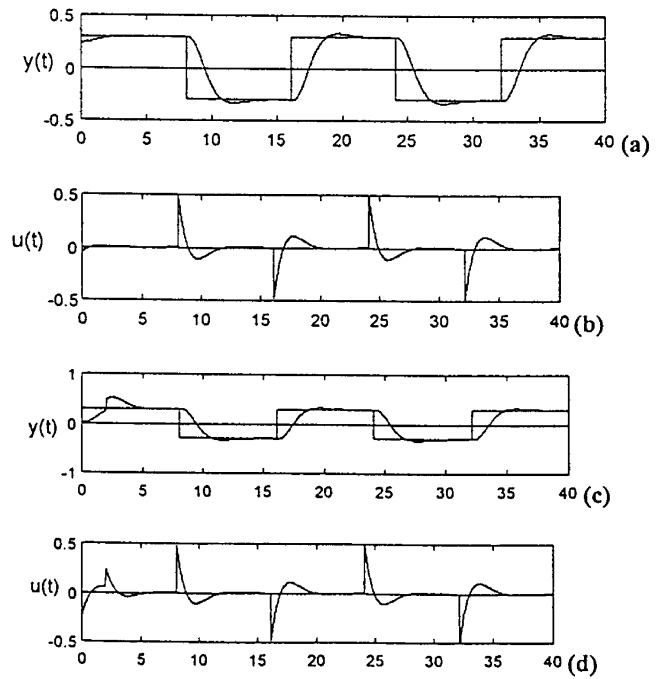


Fig. 19. Normalized responses of output and control signal by the proposed method under an additional output step disturbance of magnitude 0.24 with different starting times: (a)–(b)  $t_0 = 0$ ; (c)–(d)  $t_0 = 2$  (s).

Fig. 20(b), the maximum control signal is around 0.5. All these results coincide with the simulation performance closely. The slightly bigger overshoot was mainly due to a shift in the operating point. The unsymmetrical response was caused by the non-linearity of the plant. Strong disturbance attenuation requirements result in a larger overshoot and control effort. The performance is quite satisfactory.

## 5. Conclusion

The problem of  $H_\infty$  weighting function selection has been thoroughly investigated. Firstly, explicit multiplicative uncertainty-weighting functions have been derived for typical low-order plants with parametric uncertainties. For SISO plants with parametric uncertainties, it has been shown that an explicit uncertainty weighting function can be obtained through combinations of elementary  $PT_{1t}$ ,  $PT_{2s}$ ,  $(Ts + 1)$ ,  $\omega_n^2/(\omega_n^2 + 2d\omega_n s + s^2)$ , etc., units. Intuitively, these results could also be applied in the framework of adaptive robust design, since  $H_\infty$  weighting functions can be updated automatically as long as the interval bound of the individual parameters of a plant is given. A basic form of performance weighting functions has been suggested, with which designers could easily make trade-offs. A formula for calculating control signal weighting functions that represent the position and rate limit constraints of an actuator is given for the first

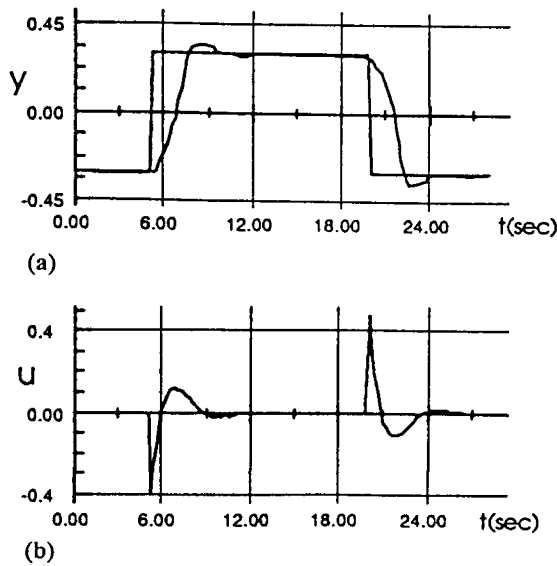


Fig. 20. (a) Real-time experimental output response with square wave input  $r = \pm 0.3$  using the proposed method. (b) Real-time experimental control signal response using the proposed method.

time. A novel  $H_\infty$ -mixed sensitivity design method is proposed to control the percentage overshoot directly. Finally, the whole procedure has been demonstrated by the roll-angle control design of a laboratory scale vertical take-off aircraft via simulation and real-time experiments. An illustrative example has shown that the transient performance of the standard  $H_\infty$  design has been significantly improved by the new technique proposed in this paper. An accurate relationship between the percentage overshoot and the weighting function established in this paper holds only when a pair of dominant poles is present in the plant. Extending the approach described here to more complex problems, including the *MIMO* case, is the subject of future research.

### Acknowledgements

Dr. Jiankun Hu is thankful to the Alexander von Humboldt Foundation (AvH) for financial support. The valuable suggestions and comments of the anonymous referees are also appreciated.

### References

- D'Azzo, J. J., & Houpis, C. H. (1995). *Feedback control system analysis & synthesis* (pp. 246–247). Tokyo: McGraw-Hill.
- Doyle, J. C., Glover, K., Khargonekar, P. P., & Francis, B. A. (1990). State space solutions to standard  $H_2$  and  $H_\infty$  control problems. *IEEE Transactions on Automatic Control*, 34, 831–847.
- Franklin, G. F., Powell, J. D., Naeni, A. E. (1994). *Feedback control of dynamic systems*. Reading, MA: Addison-Wesley Publishing Company, Inc.
- Garg, S. (1993). Robust integrated flight /propulsion control design for a STOVL aircraft using  $H_\infty$  control design techniques. *Automatica*, 29(1), 129–145.
- Garg, S., & Ouzts, P. J. (1991). Integrated flight/propulsion control design for a STOVL aircraft using  $H_\infty$  control design techniques. *Proceedings of the American control conference* (pp. 568–576).
- Hu, J., Bohn, C., & Wu, H. R. (1999). Practical  $H_\infty$  weighting functions and their applications to real-time control of a pilot plant. *Proceedings of the American control conference*, CA, USA (pp. 920–924).
- Hu, J., Unbehauen, H., & Bohn, C. (1996). A practical approach to selecting weighting functions for  $H_\infty$  control and its application to a pilot plant. *International Automatic Control Conference*, UK (pp. 998–1003).
- Kiffmeier, U. (1994). *Ein Verfahren zum Entwurf von  $H_\infty$ -optimalen Folgereglern in Frequenzbereich*. Ph.D thesis, Ruhr University Bochum.
- Kiffmeier, U., & Unbehauen, H. (1993). Design of discrete time  $H_\infty$ -optimal servo-compensators. *Proceedings of the American control conference*, USA (pp. 1062–1066).
- Knappova, V., Kiffmeier, U., & Unbehauen, H. (1995). Weighting function in  $H_\infty$ -optimal control with application to a thyristor-driven DC-motor. *Proceedings of the American control conference*, USA (pp. 3002–3006).
- Moore, B. C. (1981). Principle component analysis in linear systems: controllability, observability and model reduction. *IEEE Transactions Automatic Control*, AC-26, (pp. 17–31).
- Postlethwaite, I. S., O'Young, Gu, D.-W., & Hope, J. (1987).  $H_\infty$  control system design: A critical assessment based on industrial applications. *Proceedings of the 10th IFAC world congress*, Munich, Germany (pp. 328–333).
- Postlethwaite, I. S., Tsai, M. C., & Gu, D.-W. (1990). Weighting function selection in  $H_\infty$  design. *Proceedings of the 11th IFAC World Congress*, vol. 5, Tallin, Estonia (pp. 104–109).
- Schmid, C., & Jamshidi, M. (1996). CADACS for system analysis, synthesis, and real-time control. In P. W. Ross, *The handbook of software for engineers and scientists* (pp. 1193–1208). Boca Raton, FL: CRC Press.
- Solodownikov, W. W. (1971). *Stetige lineare systems* (pp. 568–569). Leipzig, Germany: VEB Verlag Technik Berlin.
- Yang, C. D., Ju, H. S., & Liu, W. (1994a). Experimental design of  $H_\infty$  weighting functions for flight control systems. *Proceedings of the American control conference* (pp. 2516–2520).
- Yang, C. D., Tsai, H. C., & Lee, C. C. (1994b). Systematic approach to selecting  $H_\infty$  weighting functions for DC servos. *Proceedings of the IEEE CDC* (pp. 1080–1085).